Impact of low carbon fuels (LCF) on the fuel efficiency and NOx emissions of a light-duty series hybrid commercial delivery vehicle

Antonio García*, Javier Monsalve-Serrano, David Villalta and María Guzmán-Mendoza

CMT - Motores Térmicos, Universitat Politècnica de València, Camino de Vera s/n, 46022 Valencia, Spain

Fuel 321 (2022) 124035

https://doi.org/10.1016/j.fuel.2022.124035

Corresponding author (*):

Dr. Antonio García (angarma8@mot.upv.es)

Phone: +34 963876574

Abstract

This work evaluates the potential of using four different low carbon fuels (LCF) in a series hybrid vehicle concept and compares the results to a conventional diesel combustion counterpart. To do this experimental data from a low NOx emission calibration is obtained for each of the different fuels, and 0-D vehicle simulations of an OPEL Movano van model are made to evaluate the performance, in terms of fuel consumption and engine-out NOx, during the Worldwide harmonized Light vehicles Test Cycles (WLTC) using a simplified engine map strategy. The vehicle selection allows to evaluate the scenario of a delivery application with three different payloads 0%, 50% and 100%. The work is motivated by the current automotive industry's need to reduce emissions and use energy resources efficiently, evaluating different strategies to fulfil both objectives. The evaluation of different energy sources –such as LCF– and powertrains, have been extensively researched topics, however the information is more scarce using a combination of both strategies. The results from this work show that series hybrid vehicle presents a reduction of fuel consumption of up to 5% with 100% payload, across all fuels tested. Nonetheless, engine-out emission levels of NOx show 16% worse performance for the hybrid case due to its operation at higher engine speeds and loads during the charging of the battery.

Keywords

Low carbon fuel; e-diesel; series hybrid vehicle

1 Introduction

“The future is electric” [1, 2, 3] seems to be both the slogan and a reality that has spread for the light-duty transportation sector. Electric vehicles (EV) have had steady increases in sales [4]; and their battery and general technology [5], range [6] and energy-to-weight ratio [7] have improved. In addition, emissions concerns have made EVs the preferred option for regulators regarding the 2035 scenario [8]. However, unless global regulations stablish a definitive end-date for the circulation of the internal combustion engine (ICE), combustion vehicles will still be the larger part of the current automobile fleet proportion, at least until the year 2040 [9, 10]. In other aspects, mobility has been attempted to be improved towards fewer emissions and more efficient energy distribution. In the European Union, the use of public transportation has been heavily promoted [11] and fleets of such vehicles have been proposed or converted to hybrid and electric alternatives [12]. Delivery vehicles are one of the last light-duty applications to effectively convert to electric alternatives due to factors like technology, operational costs, logistics (including recharging) and transportation capacity [13, 14], although companies such as Amazon and FedEx have included operation in some cities with fully electric vehicles in recent years [15, 16]. This last application, delivery vehicles, will be the focus of this work, studying the case of an ICE vehicle compared with a series hybrid vehicle of the same class in terms of fuel consumption and NOx emissions. A fully electric alternative is not to be compared in this work as only emissions and fuel consumption are to be assessed and, for most scenarios, driving emissions are considered non-existent for electric vehicles and energy consumption needs to be computed in equivalent terms, thus a future work regarding a complete lifecycle assessment will evaluate these aspects, including end-of-life considerations for the hybrid vehicle, the EV and the combustion vehicle.

1.1 Powertrains and energy sources

Different types of powertrains have been briefly mentioned, such as ICE vehicles, EV and hybrid vehicles. ICE vehicles are still the most widely available vehicles in circulation [17], the energy for the propulsion of these vehicles comes from the oxidation of a fuel inside the combustion chamber in the engine, and as such they emit CO2 from the burning of the fuel. In the EU, ICE passenger vehicles are responsible for around 14.5% of the total CO2 emissions (between vans and cars) which are intended to be lowered by at least 30% by the year 2030 according to Regulation (EU) 2019/631 [18]. In addition to CO2, ICE vehicles are also responsible for the emission of other pollutants. Carbon monoxide (CO), nitrogen oxides (NOx), unburned hydrocarbons (HC) and particulate matter (PM) are some of the main ones in the case of ICE vehicles and are considered criteria pollutants. These pollutants are regulated by standards likeEuro 6 [19], to prevent the hazards for the environment and live beings. To reduce criteria pollutants and CO_2 emissions from ICEs, optimizations of the engine and combustion control strategies [20, 21], as well as aftertreatment systems [22, 23] have been crucial, however in addition to these, the study of alternative sources of fuels has also been explored and improved upon [24, 25]. Among those fuels the so-called low-carbon fuels (LCF) are an alternative that can potentially reduce the CO2 emissions related to their production (as it is possible to have carbon neutral or carbon negative production) [26, 27], while at the same time it has been demonstrated that these fuels can also include some other properties that with a proper calibration can also significantly reduce criteria pollutants, as is the case with oxygenated fuels and PM emissions [28, 29]. Synthetic fuels can also serve as energy storage for intermittent sources like solar and wind [30], by converting surplus energy into a storable fuel.

Electric vehicles, use electric motors for propulsion and the energy accumulated in batteries as power sources. Hybrid vehicles, on the other hand, can use both the electric power and an ICE (depending on the configuration). The parallel configuration uses an electric machine between the ICE and the transmission without the need for a separate generator and is proven to improve fuel efficiency [31]. The series configuration (which will be the focus of this work) is the simplest configuration of hybrid electric vehicle, relying on providing traction to the wheels with a motor and generating electricity with an ICE-generator system, thus the ICE is decoupled from the vehicle speed allowing it to perform at higher efficiency [32]. Another common configuration is the power-split configuration, which is also commonly called series-hybrid, which can be subdivided depending on the arrangement between the electric motor and ICE into three types: input-split, output-split and compound-split, among whom the most popular is the input-split [33]. Hybrid vehicles add some complexity and costs to a vehicle as hardware needs to combine components from the ICE and EV [34], and control systems need to provide an optimal energy management under driving conditions [35]. In that sense, the series hybrid architecture can be favourable as its operation and optimization are simpler since the ICE-generator system is somewhat decoupled from the electric motor. Hybrid vehicles also have some advantages over ICE vehicles and EVs, as they can improve on fuel consumption while also taking advantages of strategies like regenerative braking [36], in addition to mitigate some of the range anxiety a pure EV can cause with the potential of being able to refuel as with a normal ICE vehicle.

This work, in addition to comparing the performance of the same vehicle under two different powertrain architectures (ICE and series-hybrid), will study the fuel efficiency and potential for NOx emissions reductions obtained by using LCFs with calibrations performed towards low NOx the vehicle can potentially have under the Worldwide harmonized Light vehicles Test Cycle (WLTC) on both architectures. Finally, the CO2 emissions are calculated based on the fuel consumption and carbon intensity of each of the fuels tested from the synthesis process to the use in the vehicle. In order to be able to provide driving cycle results for each of the fuels a simplified engine map methodology is used to represent the complete engine map and provide an overview of the performance of the different fuels.

2 Materials and methodology

2.1 Fuel characteristics

Four different low carbon fuels (LCFs) (LCD100, LCD66, MaxOME66 and R33) are studied in this work, and compared with a baseline European diesel case. The LCFs have renewable contents that range from 33% to 100% in volumetric composition. The number at the end of name of each fuel indicates the proportion of renewable content in their composition. Figure 1 shows the blend composition of each of the fuels. The renewable part in LCD100, LCD66 and MaxOME66 are synthetic fuels which include Fischer-Tropsch (FT) diesel and oxymethylene ethers (OMEx). R33 is a biodiesel blend with 7% fatty acid methyl esters (FAME) and 26% hydrogenated vegetable oils (HVO). The non-renewable part of the fuel blends is fossil diesel EU. The most relevant fuel properties can be seen in Table 1.

Well-to-tank carbon intensity (WTT CI) [37] is negative for LCFs, because their synthesis process can be performed with CO_2 already present in the atmosphere (without releasing new amounts from the ground) and renewable energy. This is one of the main benefits for LCFs because they can reduce lifecycle CO_2 emissions by mechanisms to capture CO_2 emissions from the atmosphere integrated into their synthesis processes (either direct carbon capture or CO_2 utilization by plants or other biological mechanisms, like the work presented in [38]). The Tank-to-Wheel carbon intensity (TTW CI) is derived from the hypothesis of complete combustion of the fuel (all the carbon in the fuel is converted into CO_2 after the combustion reaction) and represents the worst-case emission scenario for CO_2 during the engine operation. The k_{CO_2} coefficient indicates the conversion rate from the mass of the fuel to CO_2 mass. This complete combustion assumption can be justified by the high efficiencies of diesel oxidation catalyst (DOC) that help burn the by-products after the exahust [39, 40].

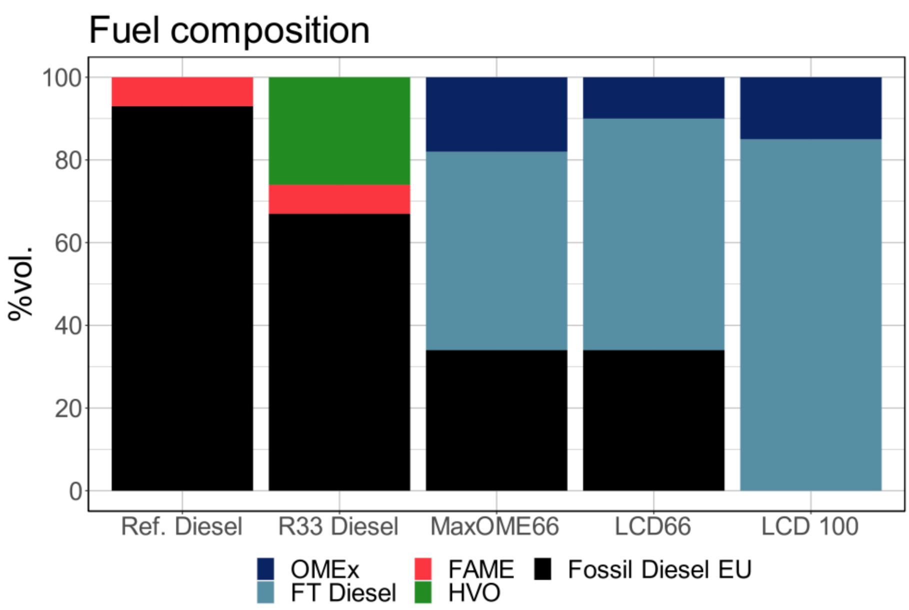

Figure 1. Fuel blend volumetric composition.

As previously mentioned, some of the fuels studied contain OMEx, whose highly oxygenated formulation and low carbon composition has been proven to be able to reduce soot emissions and provide the opportunity for low NOx calibrations [41]. OMEx fuels are synthetic, have no C-C bonds and are synthesizable using CO2 from carbon capture technology [42]. Similarly, FT provides some of the same benefits regarding its synthesis, while being the closest to conventional diesel, making it possible to blend it with conventional diesel without having to perform hardware modifications in the vehicle [43]. Finally, HVO and FAME are biofuels that can be produced from a variety of feedstock from vegetable, animal, algae, and other sources like recycled cooking oil. HVOs are a high-cetane bio-sourced mix of paraffinic hydrocarbons that lack sulphurs and aromatics, which aid in reducing NOx, unburned hydrocarbon (HC) and CO emissions, while FAMEs can have an array of properties like different cetane numbers and oxidation stability (depending on the composition) [44, 45]. Something these fuels can have in common with the increased oxygen content is a higher affinity of the blend to water molecules [45], that can lead to the faster oxidation of some engine components.

Table 1. Fuel properties at standard conditions.

Fuel	Ref. Diesel	LCD 100	LCD66	MaxOME66	R33 Diesel
Cetane Index [-]	54.6	56.6	55.6	47.4	62.4
Density @ 15ºC [g/ml]	0.834	0.821	0.825	0.8405	0.8211

Flash Point [ºC]	61	66.5	61.5	61.5	67
KV @ 40ºC [cSt]	2.86	2.08	2.23	2.074	2.904
LHV [MJ/kg]	42.81	38.67	39.96	38.24	43.04
Carbon [% m/m]	85.78	76.05	79.48	76.49	85.4
Hydrogen [% m/m]	13.45	13.81	13.78	13.3	13.84
Oxygen [% m/m]	0.77	10.14	6.75	10.21	0.76
Residue [%vol.]	1.3	1.7	1.4	1.2	1.4
kCO_2 [gCO_2/gfuel]	3.22	2.79	2.91	2.81	3.13
TTW CI [gCO_2/MJ]	75.22	72.15	72.82	73.48	72.72
WTT CI [gCO_2/MJ]	15.80	-69.20	-37.14	-36.49	-6.71

2.2 Engine characteristics and test cell description

A 4-cylinder stock 1.6 L Diesel engine was used in this investigation. More information on the engine can be found on Table 2, including the type of injectors and compression ratio. The electronic control unit (ECU) was originally provided with a baseline diesel B7 calibration used for the evaluation of the fuel blends as drop-in alternatives. Through an INCA V5.2 virtual interface 8 parameters were modified for the air management and injection systems during calibration optimization tests to achieve the desired emissions and performance targets. The parameters controlled during tests were the fuel mass injected, the injection pressure, the start of injection (SOI), the pilot injections fuel volume and dwell times, the in-cylinder cycle air mass and boosting pressure.

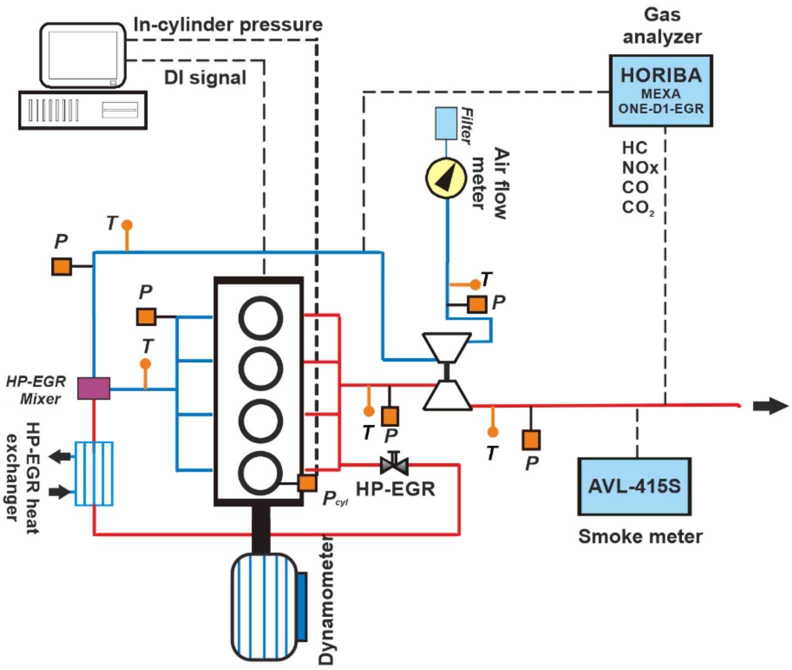

Figure 2. Test cell scheme.

Table 2. Engine characteristics.

General characteristics	
Number of cylinders [-]	4
Cylinder diameter [mm]	79.7
Stroke [mm]	80.1
Total displaced volume [cm^3]	1598
Connecting rod length [mm]	140
Compression ratio [-]	16.0
Rated power [kW]	100 @ 4000 rpm

Rated torque [Nm]	320 @ 2000 rpm
Injection system characteristics	
Type of injector	solenoid
Number of holes [-]	7
Hole diameter [μm]	141
Flow number [FN]	340
Maximum injection pressure [bar]	2000

The engine was installed in a completely instrumented test rig, provided with a Dynas$_3$ LI dynamometer to measure the torque output; a Horiba MEXA 7100 to collect information on the main engine-out emissions of interest (NOx, CO, HC, O_2 and CO_2); an AVL 415S smoke meter to measure soot in filter smoke number (FSN); an air flow meter and a fuel balance to measure fuel mass flow. Additionally, pressure and temperature probes were present at the positions identified in Figure 2 and their values were recorded by an in-house LABVIEW controller, called CMT Samaruc, which averaged the measurements. More information on the measuring equipment can be found on Table 3, including the accuracy each instrument has.

Table 3. Instrumentation accuracy.

Variable measured	Device	Manufacturer/ model	Accuracy

In-cylinder pressure	Piezoelectric transducer	Kistler / 6125C	± 1.25 bar
Intake/Exhaust pressure	Piezoresistive transducers	Kistler / 4045A	± 25 mbar
Temperature	Thermocouple	TC direct / type K	± 2.5 ºC
Crank angle, engine speed	Encoder	AVL / 364	± 0.02 CAD
NOx, CO, HC, O_2 and CO_2	Gas analyzer	Horiba MEXA 7100	4%
FSN	Smoke meter	AVL 415S	±0.025 FSN
Fuel mass flow	Fuel balance	AVL 733S	±0.2%
Air mass flow	Air flow meter	AVL 422	±0.1%
Torque	Dynamometer	$Dynas_3$ LI	

2.3 Internal combustion engine operating conditions

The selected operating conditions for this study are based on the work of [46]. These operating conditions are distributed across the engine map in such a way that they can be representative of the engine operation. The engine operating conditions are described by the labels 1250 rpm @ 2 bar, 1500 rpm @ 14 bar, 2000 rpm @ 8 bar, 2000 rpm @ 22 bar and 3750 rpm @ 18 bar which indicate the engine speed and brake mean effective pressure (BMEP).

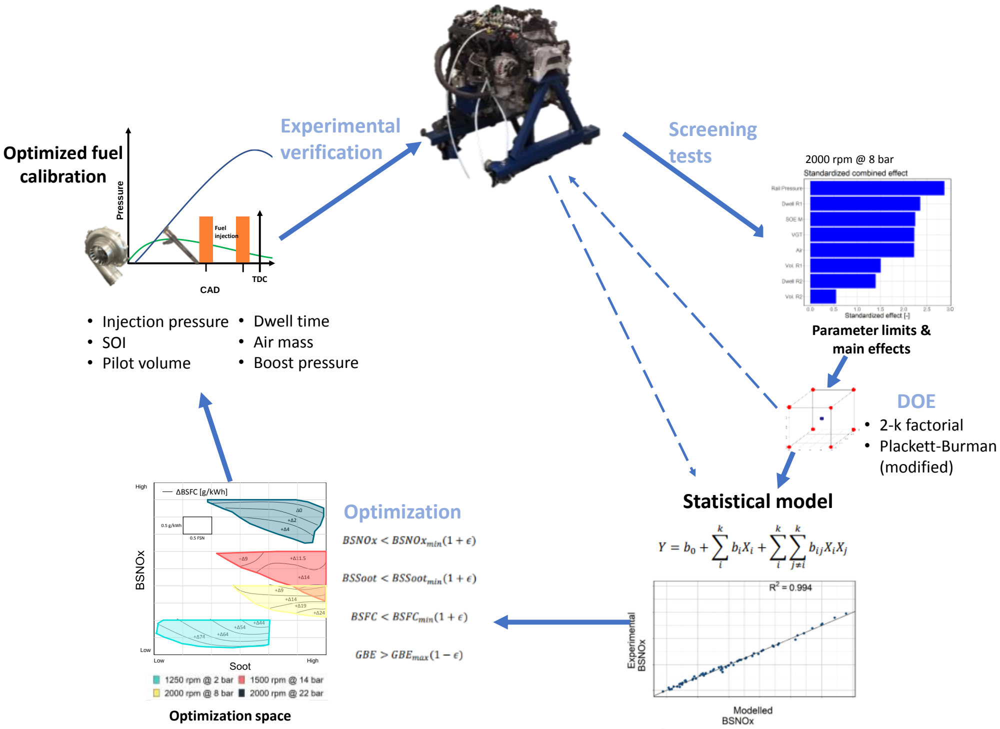

Figure 3. Summary of the calibration optimization methodology for the engine operating conditions

Each of the operating points (for each of the fuels studied) are calibrated following the methodology proposed in a previous work performed [47]. The cited methodology is synthetized by Figure 3. The first step is to perform screening tests to evaluate 8 parameters (injection pressure, SOI, pilot injection volumes, dwell time, intake air mass and boosting pressure) and reduce the number of parameters to 6. Afterwards, a design of experiments is created using either a full 2 k-factorial or a modified Placket-Burman design [48] with maximum and minimum levels, in addition to a central point. The shorter design of experiments – the Placket-Burman design – is applied to operating conditions with engine loads above 150 Nm to prevent prolonged periods of time under conditions with higher probability of excessive peak pressure, high pressure rise rate (PRR) and temperatures, but slightly reducing the fitting the model can provide for the engine condition. Subsequently, linear models are created for each operating condition and for each of the responses of interest. Among the responses that are to be given more importance in this work are the engine efficiency, fuel consumption, as well as the engine-out NOx and soot emissions. With the different models, an optimization space is created by providing values distributed within the maximum and minimum limits of the parameters and evaluating the output for the different combinations of parameters. Within this optimization space, a function to determine the combination of parameters that promotes the least number of emissions and fuel consumption with the highest possible engine efficiency is used [49]. Finally, the selected optimized operating conditions are tested in the engine, which also allows to observe the deviation between predicted and actual values. It is important to remark that during this work the value to be used for calculations in the future sections is the experimentally measured one.

2.4 Comparing the effect of different powertrains in an analogous vehicle

Two powertrain configurations are compared with the same vehicle platform, which in this case is an OPEL Movano. The vehicle is commonly used for delivery applications as it is a van with ample cargo space. The commercially available ICE model has a 2.3-liter diesel engine; however, for the purpose of this work the 1.6-liter engine defined in the previous section will be used. Accounting for the reduction of the engine size, the maximum payload is reduced from 1.2 tons to 1.1 tons as the evaluations will be made at 0%, 50% and 100% payload. The ICE vehicle will be compared with a hypothetical series-hybrid model with the same engine on-board. Additionally, the OPEL Movano model has made recently available a fully electric version with two battery sizes (37 and 70kWh) that can, reportedly, reach ranges between 116 and 247 km in the WLTP combined cycle and a payload of 1.2 tonnes [50]. Nonetheless the focus of this work are the emissions and fuel consumption that can be obtained by using the conventional ICE powertrain and the hybrid one.

2.4.1 0-D Vehicle simulation

The main characteristics of the vehicle are described on Table 4, which will be used for the 0-D vehicle model that is developed inside the GT-Suite software. The vehicle emissions reported are based on engine-out values as aftertreatment devices are not being evaluated. To compare the vehicles, the different outputs of both the ICE vehicle and the series hybrid vehicle are calculated under the WLTC. To assemble the hybrid powertrain, electric components such as battery pack, electric machines, inverters, controllers, among others, were inserted in the model driveline. In the series hybrid case, the ICE is coupled to a generator and a traction motor is coupled to the wheels by the axle and the final drive. A battery package has also been included, which increases the weight of the vehicle with respect to the ICE case and whose size depends on the final battery energy obtained after the parametric analysis. The generator is set to have the same maximum power as the ICE, while the final drive ratio is optimized in the parametric analysis due to the absence of transmission. In both the ICE and hybrid case, for the each timestep speed profile a PID controller provides the necessary power requirements for the speed demand of the WLTC.

Table 4. Vehicle characteristics for the 0-D simulation

Parameter	Architecture	Tested values
Vehicle characteristics		
Base vehicle mass [kg]	ICE; series hybrid	1950

Max. payload [kg]	ICE; series hybrid	1100
Vehicle drag coefficient [-]	ICE; series hybrid	0.65
Frontal area [m2]	ICE; series hybrid	5.18
Rolling friction [-]	ICE; series hybrid	0.0105
Tires size [mm/%/inch]	ICE; series hybrid	215/65/16
Transmission type	ICE; series hybrid	Manual
Gear shift-up [rpm]	ICE; series hybrid	2500
Gear shift-down [rpm]	ICE; series hybrid	1200
Battery pack & electric machine		
Battery size [kWh]	Series hybrid	5 – 60
Final drive ratio [-]	Series hybrid	2:1 – 12:1
SOC difference [-]	Series hybrid	2 – 25
ICE operative condition [kW]	Series hybrid	60-90
SOC start charge	Series hybrid	0.15 – 0.60
Electrical machine avg. efficiency	Series hybrid	0.85

For the calculation of fuel consumption and engine-out NOx emissions engine maps are introduced to GT-Power. Similarly, to the work performed in [47, 51], the engine maps for the LCFs are based on the 5 selected operating conditions assigning to each region of the map a different operating condition, these types of maps will be consequently called simplified maps. Among the advantages of this strategy is the possibility to be able to compare several fuels under driving cycle conditions without the need to perform a complete calibration of the engine map for each given fuel, but instead calibrate a reduced subset of engine conditions with each fuel. For the simulations, the GT-Power interpolation function was applied to the discrete map of operating conditions (both for the complete map with 48 conditions and the simplified one with 5) to allow for continuous data in terms of the load, speed and fuel consumption and NOx, respectively. Figure 4 shows the difference between the complete engine map and the simplified version after such interpolation. It is observed that although the complete map has regions with lower values the simplified map tends to average near the medium values in terms of fuel consumption. A similar case occurs with engine-out NOx emissions map. On the figure, values are expressed as an absolute difference to preserve confidential information from the OEM.

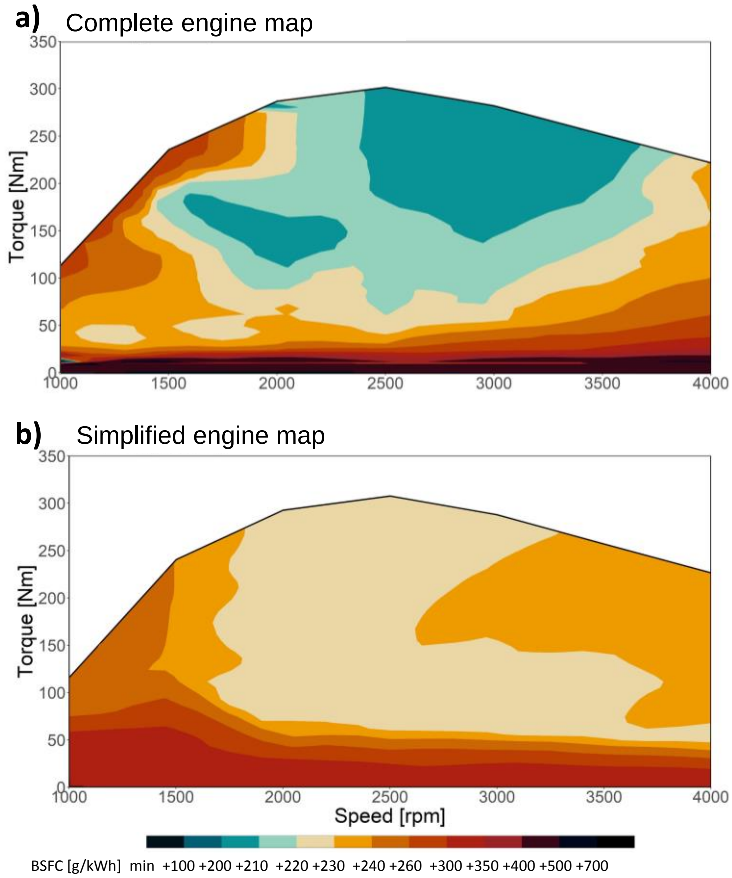

Figure 4. Brake-specific fuel consumption map for a) complete engine map and b) simplified engine map

2.4.1.1 Series hybrid vehicle parametric study

The series hybrid case has regenerative breaking and a three-level energy strategy that depends on the battery state-of-charge (SOC). In this strategy there are three established SOC levels equally separated from one another by the SOC difference parameter (in Table 4). This functioning principle generates a higher ICE power when the SOC is lowest, and vice versa. As previously mentioned, a parametric study for the series hybrid vehicle was performed to characterize the battery, control strategy and drive ratio. During this stage all simulations were performed at 50% payload and using the complete diesel ICE map. The criteria followed to select the final configuration was the reduction of the BSFC. In order to guarantee the capture of the plausible operation of the hybrid vehicle, during this study 10 consecutive cycles were simulated to account for the possibility of the battery SOC being lower at the end of the cycle than it was at the beginning. In that sense, the subsequent cycle has a starting SOC equal to the previous one's ending SOC, which allows to include in the summary analysis the effect of a discharged battery. Figure 5 shows the fuel efficiency in relation to the battery energy (which also translates into its size) in the series hybrid vehicle with 50% payload. From the left side of the figure a trend of decreasing fuel efficiency with increasing battery size can be attributed to the need for the engine to output higher power to be able to move the increased weight of the vehicle and its components caused by a battery weight that its proportional to its energy capacity. Below the 30-kWh battery range there is an area that appears to be a minimum for fuel consumption. On this initial evaluation, it was found that the optimal final drive ratio was 6. Finally, with the drive ratio fixed, the SOC difference between levels of charge for the control strategy and battery size were evaluated in the range of 5 kWh to 30 kWh (right side of Figure 5). The evaluation allowed to specify a battery size of 25 kWh with a SOC difference of 21%.

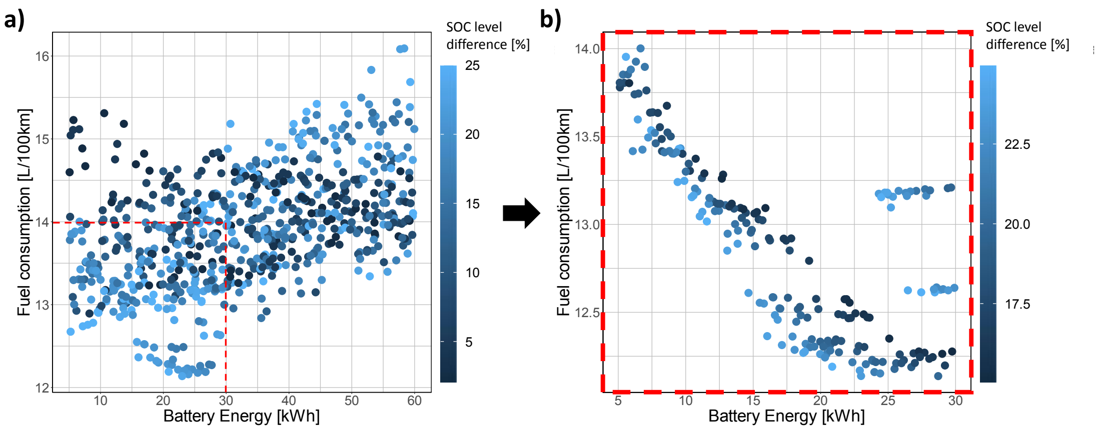

Figure 5. Battery energy vs. fuel consumption during the parametric study of the series hybrid vehicle with diesel fuel at 50% of payload

Another factor that is crucial to consider in series-hybrid vehicles is the effect the initial SOC has over the performance of the vehicle. After defining the characteristics of the hybrid vehicle an evaluation of the effect of the initial SOCs was performed in a range from 0.15 to 0.6 during one WLTC. This simple assessment provides an idea of the best- and worst-case scenarios that can be achieved in terms of fuel efficiency and NOx emissions in the series-hybrid case, with the same configuration. Figure 6 a to c show the variation through time of the WLTC vehicle speed profile, and whether the ICE is activated or not and how the SOC changes over the cycle. The blue line in the figure indicates the mean values so a general trend is easier to notice (for the case of ICE engine on/off plot it indicates what percentage of cases have the ICE on at a given timestep). One important observation to be made is that regardless of the initial SOC, the end SOC does not surpass 0.40 because although the ICE is engaged in operation for the majority of cases after 1000 seconds, the energy from the battery and the engine has to be both able to move the vehicle and have enough excess quantity to recharge the battery during the higher vehicle speed section of the driving cycle, which typically requires the highest energy already. This will have an important effect in the future sections as the hybrid vehicle is evaluated on a ten-cycle basis, which implies that if the initial SOC is 0.6, the following ones will necessarily have a starting SOC below that value. Elements d and e from Figure 6 show the cumulative fuel and NOx emissions during the cycle, showing how the higher speed sections of the cycle contribute the highest proportion of emissions and fuel consumption, coinciding with previous conclusions that indicate that hybrid vehicles are better suited to urban driving patterns instead of highway driving patterns [52, 53, 54]. Precisely, at the low and medium sections of the WLTC the average fuel consumption is only 1/8 of the total average and the NOx emissions 1/9 of the final average. In that sense, as the intended vehicle is a cargo van for package delivery interurban driving is their main use case, implying a lower rate of fuel consumption and engine-out emissions of NOx.

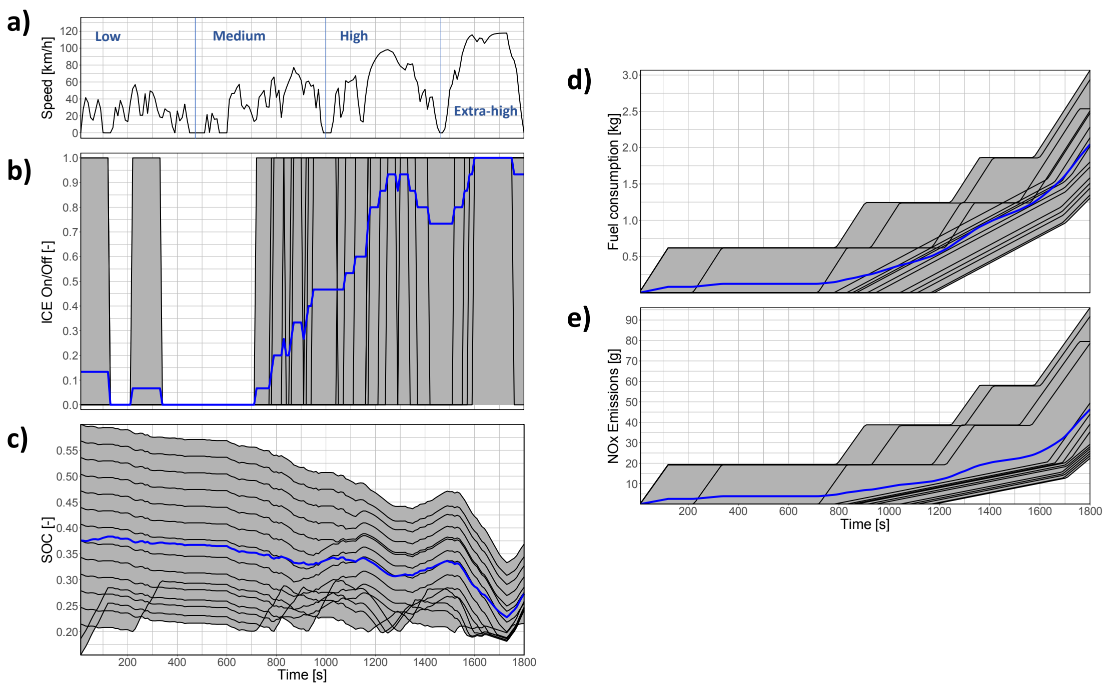

Figure 6. Instantaneous variation during the WLTC of the a) vehicle speed, b) ICE on/off activation, c) SOC, d) fuel consumption and e) engine-out NOx emissions

Finally, the direct correlation between the starting SOC and the ending SOC, fuel efficiency and engine-out NOx emissions can be seen in Figure 7. The positive correlation between the value of the starting SOC and the end SOC can be more easily observed, as well as the decrease of engine-out NOx emissions and fuel consumption in a seemingly quadratic form. With this information, the case with 0.6 initial SOC is easily identifiable as the best-case scenario, which in future sections will be used to know the minimum value for the emissions and fuel consumption of the hybrid vehicle.

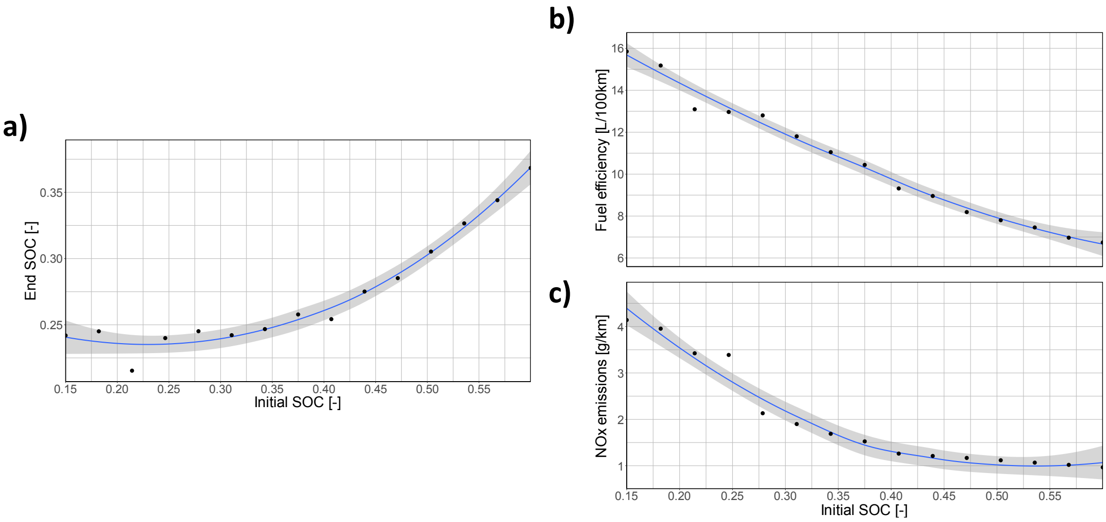

Figure 7. Initial SOC effect on a) End SOC; b) Fuel efficiency; c) NOx emissions

2.4.1.2 Error analysis of using a simplified engine map strategy

To validate the use of a simplified engine map in the prediction of engine-out NOx emissions and fuel consumption calculations, the simplified diesel engine map was compared to the complete diesel engine map for all payloads. In addition, the difference in the results between one type of map and the other will be used as the error for the ICE vehicle model in future sections. Figure 8 shows the fuel consumption for the hybrid and the ICE vehicle models. In the case of the cumulative fuel consumption a good relation can be observed between the simplified and the complete map, maintaining the total error percentage (defined as the difference between both cases divided by the complete map value) below 7%. In the case of the hybrid vehicle the complete and simplified map also show good correlation with one another while maintaining an error below 6%. The hybrid vehicle results also include the SOC through the cycle as it was previously established how the initial value affects fuel consumption and emissions due to the need for more powerful engine outputs. From the figure, it can also be observed how the ICE and hybrid vehicle compare when the battery is partially discharged at the beginning of the cycle. At low vehicle speed the engine in the ICE vehicle operates at low engine speeds and loads consuming a low mass flow rate of fuel, contrarily as the battery of the hybrid vehicle needs recharging at the beginning of the cycle, the fuel mass flow rate is higher translating into around 1500 g of fuel used at the time point (400 seconds) where the ICE model has only used around 250 g of fuel. Later, when the fuel consumption plateaus in the hybrid vehicle from the time point 400 seconds to around 1200 seconds due to the engine being off, the fuel consumption remains higher than the ICE case. It is important to remark, however, that the currently shown case is one of the worst-case scenarios for the initial SOC in the hybrid vehicle, and thus there are cycles with more favourable SOCs that have better fuel efficiency.

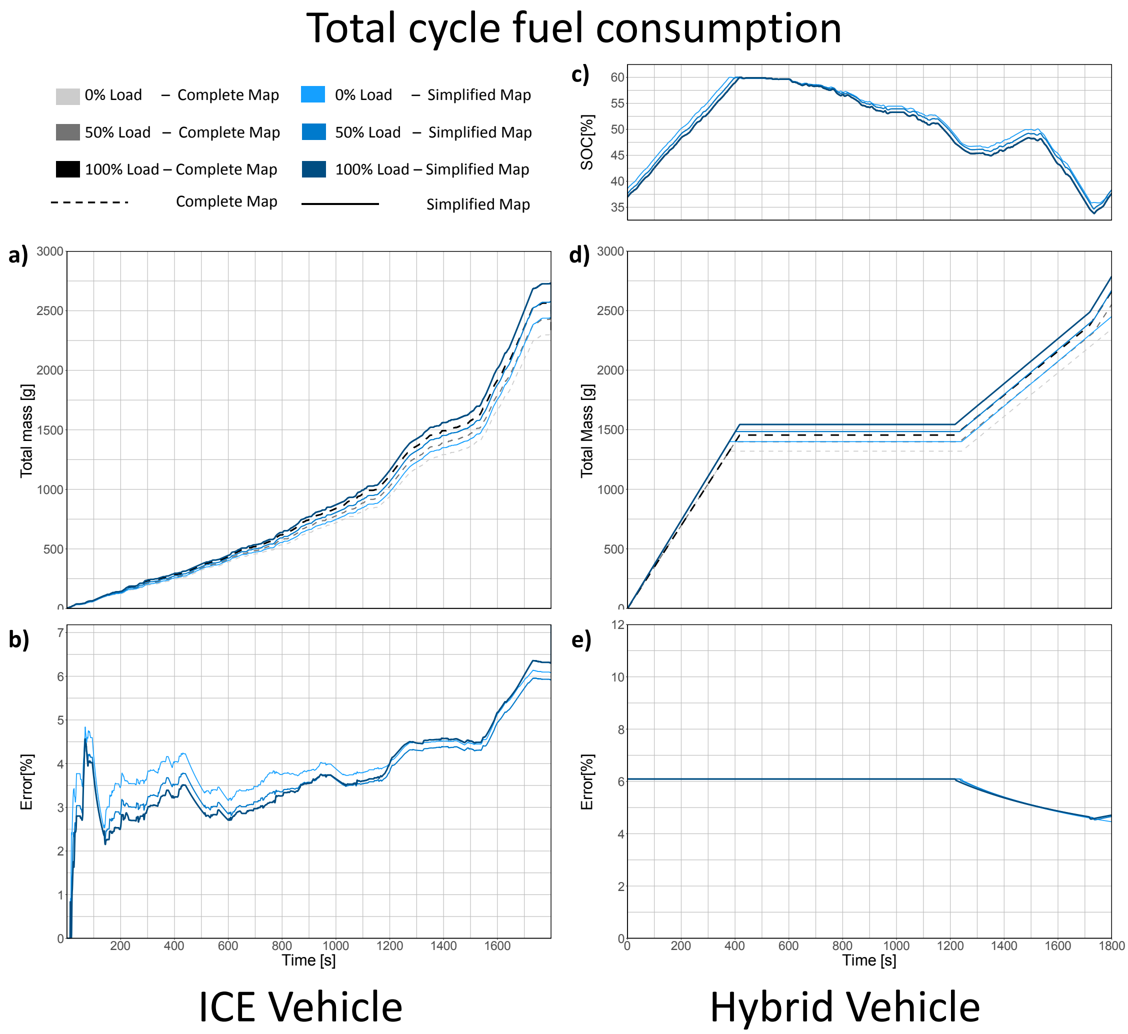

Figure 8. Instantaneous results for the complete and simplified engine maps with 50% payload and diesel fuel for: a) cumulative fuel consumption for the ICE vehicle; b) fuel consumption error for the ICE vehicle; c) SOC for the series-hybrid vehicle; d) cumulative fuel consumption for the series-hybrid vehicle; e) fuel consumption error for the series-hybrid vehicle.

Figure 9 shows the total NOx emissions evolution through the WLTC cycle. Similar to the fuel consumption, the engine-out NOx emissions obtained by using the simplified map show good correlation to the use of the complete map. After an initial high difference between maps in the ICE vehicle case, the relative error then remains mostly in values below 5%. On the other hand, the hybrid vehicle error between maps is constantly below 7.5% with a decrease in the high and extra-high sections of the WLTC cycle as engine-out NOx emissions for both cases increase, while the absolute engine-out NOx difference (the subtraction of the complete map engine-out NOx result minus the simplified map result) remains seemingly constant. Comparing the cycle for the ICE vehicle and series hybrid vehicle model (with near 37% of initial SOC), provides similar conclusions for the NOx emissions as the ones obtained for the fuel consumption, where the hybrid vehicle is much faster at reaching a higher quantity of engine-out NOx.

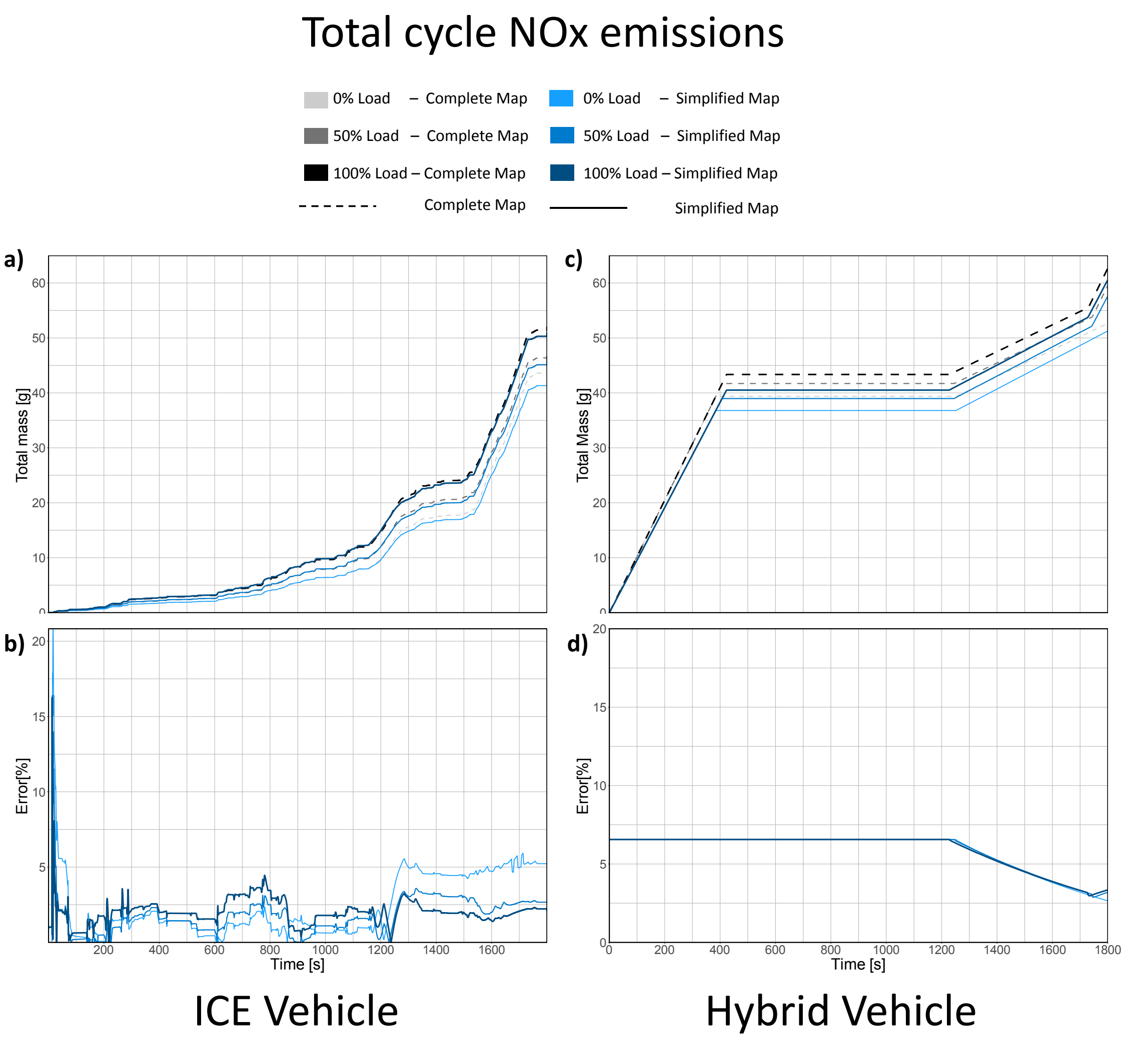

Figure 9. Instantaneous results for the complete and simplified engine maps with 50% payload and diesel fuel for: a) cumulative engine-out NOx emissions for the ICE vehicle; b) engine-out NOx emissions error for the ICE vehicle; c) cumulative engine-out NOx emissions for the series-hybrid vehicle; e) engine-out NOx emissions error for the series-hybrid vehicle

3 Performance and emissions results with LCF

Parameter	Architecture	Values
Vehicle characteristics		
Base vehicle mass [kg]	ICE; series hybrid	1950
Max. payload [kg]	ICE; series hybrid	1100
Vehicle drag coefficient [-]	ICE; series hybrid	0.65
Frontal area [m2]	ICE; series hybrid	5.18
Rolling friction [-]	ICE; series hybrid	0.0105
Tires size [mm/%/inch]	ICE; series hybrid	215/65/16
Transmission type	ICE; series hybrid	Manual
Gear shift-up [rpm]	ICE; series hybrid	2500
Gear shift-down [rpm]	ICE; series hybrid	1200
Internal combustion engine		
Number of cylinders [-]	ICE; series hybrid	4
Cylinder diameter [mm]	ICE; series hybrid	79.7
Stroke [mm]	ICE; series hybrid	80.1
Total displaced volume [cm^3]	ICE; series hybrid	1598
Connecting rod length [mm]	ICE; series hybrid	140
Compression ratio [-]	ICE; series hybrid	16
Rated power [kW]	ICE; series hybrid	100 @ 4000 rpm
Rated torque [Nm]	ICE; series hybrid	320 @ 2000 rpm
Battery pack & electric machine		
Battery size [kWh]	Series hybrid	25
Final drive ratio [-]	Series hybrid	6:1
SOC difference [-]	Series hybrid	21
ICE operative condition [kW]	Series hybrid	60-90
SOC start charge	Series hybrid	0.15 – 0.60
Electrical machine avg. efficiency	Series hybrid	0.85

As described in the methodology section, this work comprises the evaluation of four LCFs in a series hybrid and ICE vehicle model whose intended purpose is package delivery and compares the potential of using one platform or the other under the WLTC. The final vehicle characteristics are summarized in . Figure 10 shows the fuel efficiency, engine-out NOx emissions and tailpipe CO_2 emissions for the 0%, 50% and 100% payload cases with different LCFs under the WLTC cycle. In the hybrid vehicle case, the value is the average after performing 10 consecutive cycles while the error bars show the maximum and minimum possible values achievable under only one cycle depending on the starting SOC of that cycle (as that is the biggest possible error magnitude). In the case of the ICE vehicle, the error bar shows the variability allowable by using a simplified engine map instead of the complete map. Regarding energy demands, the use of a hybrid vehicle can allow an average increase of fuel efficiency of 1.97%, 3.85% and 5% for the 0%, 50% and 100% payload cases, respectively, regardless of the fuel used. It can also be noted how fuel consumption increases as renewable content increases (also related to the decrease of carbon content in the fuel and thus the energy density in the fuel). The fuels with higher OMEx content have in general the worst fuel consumption, while R33 – an energy dense biodiesel – has a fuel consumption that is similar to that of the reference diesel. The other notable result is that for the hybrid vehicle, increasing from 0% payload to 50% payload increases the fuel consumption 3.29 – 4.27%, while for the ICE vehicle has a penalty of 5.50 – 5.79% for the same increase of payload. Conversely, when increasing the payload from 50% to 100% the hybrid vehicle sees an average increase of 5.02% while the ICE increases by 6.29%. Finally, if evaluating only the best-case scenario cycle for the hybrid vehicle a further reduction of 5 L/100km could be achieved. Although the hybrid vehicle improves on fuel efficiency, it does on average only by a small margin, and only the cases with initial SOCs higher than 0.6 would have fuel efficiency savings in the order of 30% to 40% (similar to other studies [55]). This is because, when the cycle starts with a lower SOC, during most of the cycle the ICE engine is in the on state at higher engine speeds and loads to produce the necessary power to simultaneously propel the vehicle and charge the battery, causing a higher fuel consumption than in a case where the initial SOC is high and the vehicle operates with only the electric machine and battery.

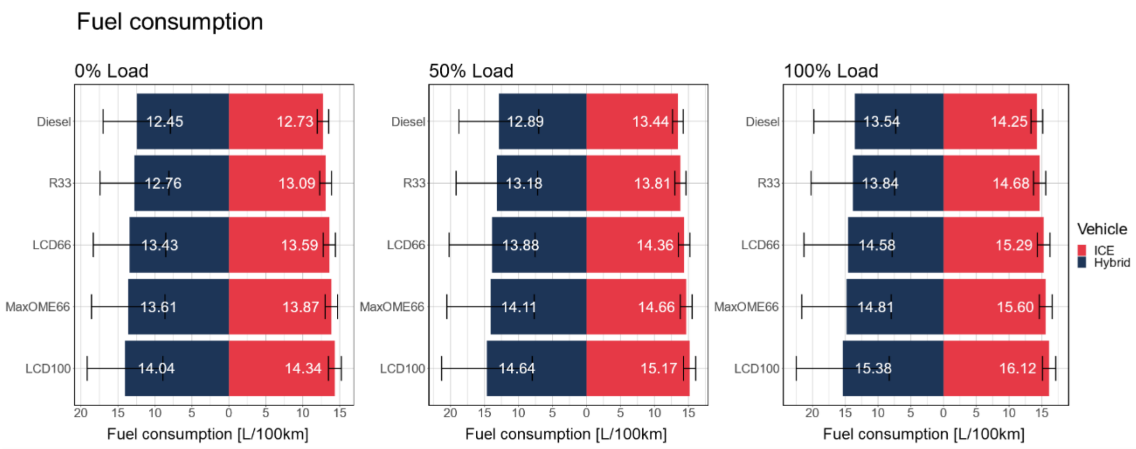

Figure 10. Fuel consumption results for the WLTC with different LCF compared to diesel at 0%, 50% and 100% payload

Engine-out NOx emissions on Figure 11 show an opposed trend to the fuel consumption, with the series hybrid vehicle presenting an average of 16% higher NOx emissions by kilometer than the ICE vehicle (except for the diesel fuel, which has similar values in both vehicles). This can be mainly attributed to the hybrid vehicle operating a higher percentage of the time on higher engine load and speed conditions than the ICE model. The high-renewable-content highly oxygenated fuels like LCD100 and MaxOME66 have non-sooting capabilities that allowed for a calibration which significantly increased the EGR levels without exceeding imposed soot limit [56], thus reducing engine-out NOx. Although the R33 and LCD66 fuels are not the best performing fuels in terms of engine-out NOx, they still present an improvement of 0.5 g/km over diesel fuel. None of the fuels under any payload or vehicle type achieve the Euro 6 limit of 0.06 g/km for light commercial vehicles with their engine-out emissions, not even the most favourable hybrid vehicle case which can reduce emissions by 0.5 g/km from the average. However, it is not unreasonable to think that it is possible to reach Euro

6 with the integration of a three-way catalytic converter as an aftertreatment device to reduce tailpipe NOx.

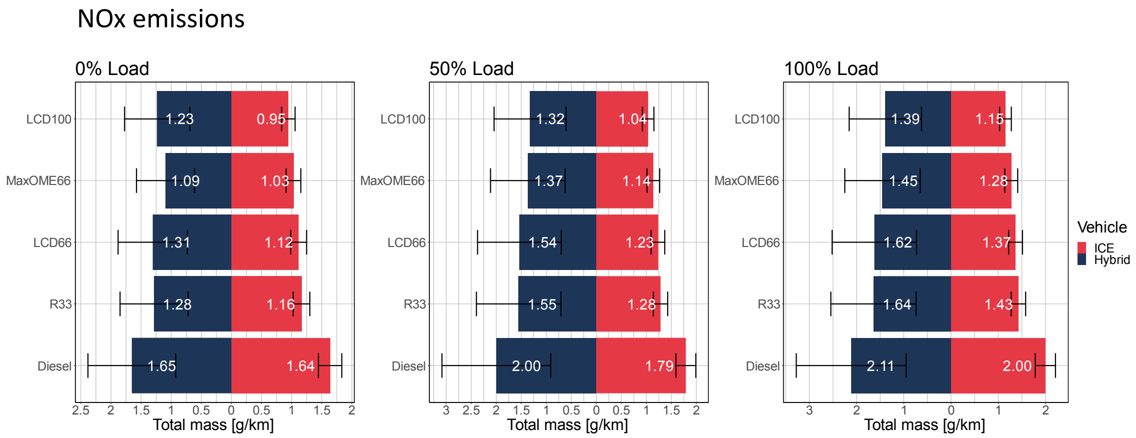

Figure 11. Engine-out NOx emissions results for the WLTC with different LCF compared to diesel at 0%, 50% and 100% payload

One of the main selling points for the study of LCFs is the potential for CO_2 emission reductions in their lifecycle analysis because their synthesis process can use recycled CO_2 instead of new resources and the energy used for the process is ideally completely renewable. With that in mind, using the WTT and TTW carbon intensity values from Table 1 the CO_2 emissions were calculated and presented on Figure 12, in addition to WTW emissions. For this work, TTW are obtained assuming the hypothesis of complete combustion which implies that all the carbon from the fuels reacts forming CO_2. TTW CO_2 emissions are very close among the fuels because the fuels with the higher fuel consumption present slightly lower CI values and thus the result is balanced among fuels. The really important difference comes from the WTT emissions, where the renewable fuels have negative values which indicate that theoretically the CO_2 emissions derived from their synthesis are lower than the CO_2 captured for the process (in the figure the elements with a striped pattern). Then, the WTW emissions are the result of adding the TTW and WTT emissions. Thus, the higher the renewable content of the fuel shows the highest potential for CO_2 reduction of net emissions from the lifecycle of the fuel. This can be observed in Figure 12 with the progressive reduction of WTW emissions as the renewable content of the fuel increases until LCD100 has only 5% of the CO_2 emissions of the diesel fuel for both the hybrid and ICE vehicle case. In terms of comparing the hybrid vehicle model to the ICE one, CO_2 emissions are reduced in the same proportion as the fuel consumption, which translates into a reduction of around 20 g/km for the hybrid vehicle.

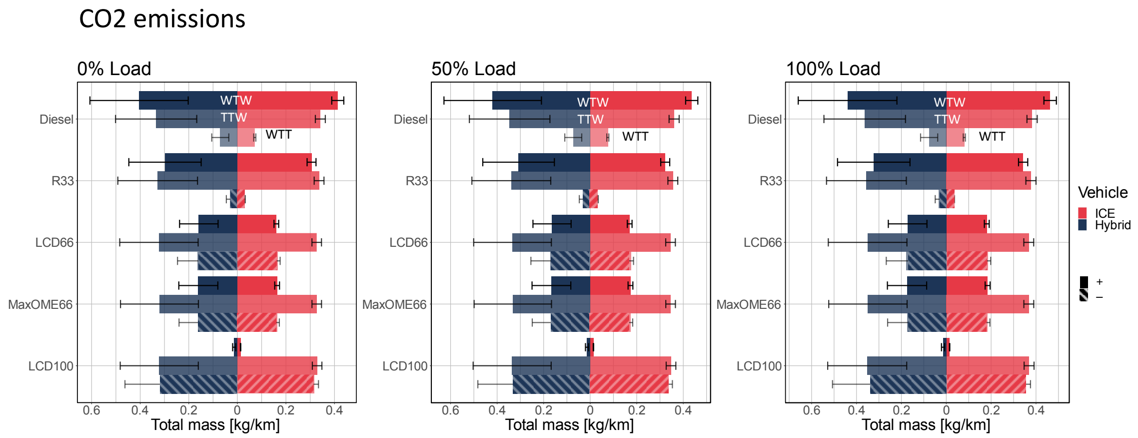

Figure 12. WTT, TTW and WTW CO2 emission results for the WLTC with different LCF compared to diesel at 0%, 50% and 100% payload. (Striped bars indicate carbon negative values)

4 Summary and conclusions

This work evaluated an ICE and series hybrid OPEL Movano van with three different payloads under the WLTC with GT-Power 0-D model cycle to assess the fuel consumption and engine-out NOx emissions of four LCFs compared to diesel as the reference. For the evaluation of the LCFs a simplified engine map strategy was described and applied which allows the calibration of the operation with LCFs, without the time and resource consuming task of calibrating the entire engine map with each of the fuels allowing to provide an overview of the advantages of each fuel with limited quantities and provide insight on the fuel with more potential for further study. Before being able to compare the vehicles, a parametric study was performed for the series hybrid vehicle to characterize the battery size, the final drive ratio and the SOC difference between levels of SOC. After that study, due to high dependency of the performance of the vehicle with the starting SOC, a sweep study was performed with the starting SOC and ending SOC, engine condition, fuel consumption and engine-out NOx emissions. Finally, the results were summarized to compare the two different platforms with all the LCFs, including the CO_2 emissions in terms of WTT, TTW and WTW. The main findings of this work are summarized as follows:

- When considering more than one consecutive WLTC cycles (to account for different initial SOC), battery sizes above 30 kWh have fuel consumptions above 13 L/100km for the series hybrid vehicle model using the selected 1.6 L engine.
- In the series hybrid vehicles, the starting SOC is one of the more influential factors in determining the performance of the vehicle. Starting SOC above 0.4 have fuel consumptions below 10 L/100km and engine-out NOx emissions that do not reach 1.2 g/km. Nonetheless the ending SOC of one WLTC does not reach a value above 0.4, so any consecutive cycle starts with values below this number.
- Engine-out NOx emissions and fuel consumption are inversely correlated to the initial SOC. Regarding the rate of increase, these values rise the fastest during the High and Extra-high phases of the WLTC.
- The simplified engine map strategy can provide comparable results to the complete engine map at the end of the cycle with a maximum error for

6.5% for the fuel consumption and 7% for the engine-out NOx emissions for both the series hybrid and ICE vehicle models.

- Fuel consumption for the series hybrid vehicle is on average 3.6% lower than the ICE vehicle across all fuels.
- Fuels with higher proportion of renewable content, due to their lower energy dense composition, have worse fuel consumption than diesel in both vehicle cases. This is exacerbated in the cases with higher OMEx proportions.
- Engine-out NOx emissions are not improved by the use of a series hybrid vehicle. Even using fuels with a high OMEx content, whose operation calibration allows to significantly increase the EGR to reduce this emission without promoting significant soot reach levels above 1 g/km in engine-out emissions.
- The series-hybrid vehicle results are not significantly better than the ICE model results. Making unable to currently justify the added weight and cost of using a series electric vehicle under normal applications. Nonetheless, due to the observed rate of increase in emissions and fuel consumption during the different phases of the WLTC, it is considered that during driving patterns that are exclusively urban and interurban this type of vehicles would present bigger advantages with respect to the ICE model, such as delivery routes for postal services. Such service specific routes are a topic to be evaluated in future studies particularly under the fuel LCD66 which present a good trade-off between fuel consumption and NOx emissions.

Acknowledgments

The authors thank ARAMCO Overseas Company for supporting this research.

References

[1] J.P. Morgan, "The Future is Electric," J.P. Morgan, [Online]. Available: https://www.jpmorgan.com/insights/research/future-is-electric. [Accessed 9 October 2021].

[2] McKinsey & Company, "Why the automotive future is electric," 7 September 2021. [Online]. Available: https://www.mckinsey.com/industries/automotive-and-assembly/our-insights/why-the-automotive-future-is-electric. [Accessed October 2021].

[3] Queensland Government, "The Future is Electric - Queensland's Electric Vehicle Strategy," 11 October 2017. [Online]. Available: https://www.publications.qld.gov.au/dataset/the-future-is-electric-queensland-s-electric-vehicle-strategy/resource/7e352dc9-9afa-47ed-acce-2052cecfec8a. [Accessed October 2021].

[4] T. Gersdorf, P. Schaufuss, S. Schenk and P. Hertzke, "McKinsey Electric Vehicle Index: Europe cushions a global plunge in EV sales," July 2020. [Online]. Available: https://www.mckinsey.com/~/media/McKinsey/Industries/Automotive%20and%20Assembly/Our%20Insights/McKinsey%20Electric%20Vehicle%20Index%20Europe%20cushions%20a%20global%20plunge%20in%20EV%20sales/McKinsey-Electric-Vehicle-Index-Europe-cushions-a-global-plun. [Accessed 10 April 2021].

[5] Z. Liu, J. Song, J. Kubal, N. Susarla, K. W. Knehr, E. Islam, P. Nelson and S. Ahmed, "Comparing total cost of ownership of battery electric vehicles and internal combustion engine vehicles," *Energy Policy,* vol. 158, p. 112564, 2021.

[6] Y. Zhou, R. Wen, H. Wang and H. Cai, "Optimal battery electric vehicles range: A study considering heterogeneous travel patterns, charging behaviors, and access to charging infrastructure," *Energy,* vol. 197, p. 116945, 2020.

[7] Y. Zeng, D. Chalise, s. D. Lubner, S. Kaur and R. S. Prasher, "A review of thermal physics and management inside lithium-ion batteries for high energy density and fast charging," *Energy Storage Materials,* vol. 41, pp. 264-288, 2021.

[8] European Comission, *Proposal for a REGULATION OF THE EUROPEAN PARLIAMENT AND OF THE COUNCIL amending Regulation (EU) 2019/631 as regards strengthening the CO2 emission performance standards for new passenger cars and new light commercial vehicles in line with the Union's inc,* Brussels: European Comission, 2021.

[9] A. Arora, N. Niese, E. Dreyer, A. Waas and A. Xie, "Why Electric Cars Can't Come Fast Enough," BCG, 20 April 2021. [Online]. Available: https://www.bcg.com/publications/2021/why-evs-need-to-accelerate-their-market-penetration.

[10] IEA, "Global EV Outlook 2021," IEA, Paris, 2021.

[11] V. Barros, C. Oliveira Cruz, T. Júdice and J. Miranda Sarmento, "Is taxation being effectively used to promote public transport in Europe?," *Transport Policy,* vol. 114, no. December 2021, pp. 215-224, 2021.

[12] A. García, J. Monsalve-Serrano, R. Lago Sari and S. Tripathi, "Life cycle CO_2 footprint reduction comparison of hybrid and electric buses for bus transit networks," *Applied Energy,* vol. 308, no. February, p. 118354, 2022.

[13] S. Pelletier, O. Jabali and G. Laporte, "Goods distribution with electric vehicles: review and research perspective," *Technical Report CIRRELT-2014-44,* 2014.

[14] G. Napoli, A. Polimeni, S. Micari, G. Dispenza, V. Antonucci and L. Andaloro, "Freight distribution with electric vehicles: A case study in Sicily. Delivery van development," *Transportation Engineering,* vol. 3, no. March, p. 100048, 2021.

[15] A. J. Hawkins, "FedEx receives its first electric delivery vans from GM's BrightDrop," The Verge, 2021.

[16] Amazon Staff, "Amazon's custom electric delivery vehicles are starting to hit the road," Amazon, 2021.

[17] IEA, "Global EV Outlook 2021," IEA, Paris, 2021.

[18] European Comissio, "CO_2 emission performance standards for cars and vans," European Comissions, 2021. [Online]. Available: https://ec.europa.eu/clima/eu-action/transport-emissions/road-transport-reducing-co2-emissions-vehicles/co2-emission-performance-standards-cars-and-vans_en. [Accessed 03 January 2022].

[19] *Regulation (EC) No 715/2007 of the European Parliament and of the Council of 20 June 2007 on type approval of motor vehicles with respect to emissions from light passenger and commercial vehicles (Euro 5 and Euro 6),* EUR-Lex, 2020.

[20] A. Omanovic, N. Zsiga, P. Soltic and C. Onder, "Increased Internal Combustion Engine Efficiency with Optimized Valve Timings in Extended Stroke Operation," *Energies,* vol. 14, no. 10, p. 2750, 2021.

[21] A. García, J. Monsalve-Serrano, R. Lago Sari and Á. Fogué-Robles, "Use of EGR e-pump for Dual-Mode Dual-Fuel engines in mild hybrid architectures," *Energy Conversion and Management,* vol. 247, no. November, p. 114701, 2021.

[22] P. Piqueras, A. García, J. Monsalve-Serrano and M. J. Ruiz, "Performance of a diesel oxidation catalyst under diesel-gasoline reactivity controlled compression ignition combustion conditions," *Energy Conversion and Management,* vol. 196, no. September, pp. 18-31, 2019.

[23] A. Gambarotta, V. Papetti and P. Dimopoulos Eggenschwiler, "Analysis of the Effects of Catalytic Converter on Automotive Engines Performance Through Real-Time Simulation Models," *Front. Mech. Eng.,* vol. 5, p. 48, 2019.

[24] G. Kumar, S.-H. Kim, C.-H. Lay, K. Ponnusamy and Vinoth, "Recent developments on alternative fuels, energy and environment for sustainability," *Bioresource Technology,* vol. 317, no. December, p. 124010, 2020.

[25] H. Stančin, H. Mikulčića, X. Wang and N. Duić, "A review on alternative fuels in future energy system," *Renewable and Sustainable Energy Reviews,* vol. 128, no. August, p. 109927, 2020.

[26] C. Fernández-Dacosta, L. Shen, W. Schakel, A. Ramirez and G. J. Kramer, "Potential and challenges of low-carbon energy options: Comparative assessment of alternative fuels for the transport sector," *Applied,* vol. 236, no. February, pp. 590-606, 2019.

[27] J. Lepitzki and J. Axsen, "The role of a low carbon fuel standard in achieving long-term GHG reduction targets," *Energy Policy,* vol. 119, no. August, pp. 423-440, 2018.

[28] J. Han, S. Wang, R. M. Vittori and L. Somers, "Experimental study of the combustion and emission characteristics of oxygenated fuels on a heavy-duty diesel engine," *Fuel,* vol. 268, no. May, p. 117219, 2020.

[29] P. Verma, M. Jafari, S. A. Rahman, E. Pickering, S. Stevanovic, A. Dowell, R. Brown and Z. Ristovski, "The impact of chemical composition of oxygenated fuels on morphology and nanostructure of soot particles," *Fuel,* vol. 259, no. January, p. 116167, 2020.

[30] D. Candelaresi and G. Spazzafumo, "1 - Introduction: the power-to-fuel concept," *Power to Fuel, How to Speed Up a Hydrogen Economy,* pp. 1-15, 2021.

[31] J. Benajes, A. García, J. Monsalve-Serrano and S. Martínez-Baggio, "Optimization of the parallel and mild hybrid vehicle platforms operatng under conventional and advanced combustion modes," *Energy Conversion and Management,* vol. 190, no. February, pp. 73-90, 2019.

[32] C. Ji, B. Wang and Z. X. Liu, "Emissions performance of a hybrid hydrogen-gasoline engine-powered passenger car under the New European Driving Cycle," *Fuel,* vol. 106, pp. 873-875, 2013.

[33] A. García, J. Monsalve-Serrano, S. Martinez-Boggio and P. Gaillard, "Impact of the hybrid electric architecture on the performance and emissions of a delivery truck with a dual-fuel RCCI engine," *Applied Energy,* vol. 301, p. 117494, 2021.

[34] M. Weiss, A. Zerfass and E. Helmers, "Fully electric and plug-in hybrid cars - An analysis of learning rates, user costs, and costs for mitigating CO2 and air pollutant emissions," *Journal of Cleaner Production,* vol. 212, no. March, pp. 1478-1489, 2019.

[35] W. Enang and C. Bannister, "Modelling and control of hybrid electric vehicles (A comprehensive review)," *Renewable and Sustainable Energy Reviews,* vol. 74, no. July, pp. 1210-1239, 2017.

[36] A. García and J. Monsalve-Serrano, "Analysis of a series hybrid vehicle concept that combines low temperature combustion and biofuels as power source," *Results in Engineering,* vol. 1, no. March, p. 100001, 2019.

[37] M. Yugo, V. Gordillo, E. Shafiei and A. Megaritis, "A look into the life cycle assessment of passenger cars running on advanced fuels," in *SIA Powertrain & Electronics conference*, France, 2021.

[38] U. K. Roy, T. Radu and J. L. Wagner, "Carbon-negative biomethane fuel production: Integrating anaerobic digestion with algae-assisted biogas purification and hydrothermal carbonisation of digestate," *Biomass and Bioenergy,* vol. 148, no. May, p. 106029, 2021.

[39] J. Benajes, A. García, J. Monsalve-Serrano and R. Sari, "Evaluating the Efficiency of a Conventional Diesel Oxidation Catalyst for Dual-Fuel RCCI Diesel Gasoline Combustion," *SAE Technical Paper,* vol. 01, no. Sept, p. 1729, 2018.

[40] A. Ayodhya and K. Narayanappa, "An overview of after-treatment systems for diesel engines," *Environ Sci Pollut Res Int,* vol. 25, no. 35, pp. 35034-35047, 2018.

[41] A. García, J. Monsalve-Serrano, D. Villalta and Á. Fogué-Robles, "Evaluating OMEx combustion towards stoichiometric conditions in a compression ignition engine," *Fuel,* vol. 303, p. 121273, 2021.

[42] J. Benajes, A. García, J. Monsalve-Serrano and S. Martínez-Boggio, "Potential of using OMEx as substitute of diesel in the dual-fuel combustion mode to reduce the global CO2 emissions," *Transp. Eng.,* vol. 1, p. 100001, 2020.

[43] S. Hänggi, P. Elbert, T. Bütler, U. Cabalzar, S. Teske, C. Bach and C. Onder, "A review of synthetic fuels for passenger vehicles," *Energy Reports,* pp. 555-569, 2019.

[44] H. Aatola, M. Larmi, T. Sarjovaara and S. Mikkonen, "Hydrotreated Vegetable Oil (HVO) as Renewable Diesel Fuel: Trade-off betweeen NOx, Particulate Emission, and Fuel Consumption of a Heavy Duty Engine," *SAE Int. J. Engines,* vol. 1, no. 1, pp. 1251-1262, 2009.

[45] A. Dahiya, "Chapter 31 - Cutting-edge biofuel conversion technologies to integrate into petroleum-based infrastructure and integrated biorefineries," in *Bioenergy*, Second Edition ed., 2020, pp. 649-670.

[46] R. Durrett and M. Potter, "Renewable Energy to Power through Net-Zero-Carbon Fuels," in *THIESEL 2020 Conference on Thermo- and Fluid Dynamic Processes in Direct Injection Engines 8th-11th September 2020*, Valencia, 2020.

[47] A. García, J. Monsalve-Serrano, D. Villalta and M. Guzmán-Mendoza, "Optimization of low carbon fuels operation on a CI engine under a simplified driving cycle for transportation de-fossilization," *Fuel,* vol. 310, no. Part A, p. 122338, 2022.

[48] Analytical Methods Committee AMCTB No 55, "Experimental design and optimisation (4): Plackett–Burman designs," *Anal. Methods,* vol. 5, no. 8, pp. 1901-1903, 2013.

[49] A. García, J. Monsalve-Serrano, D. Villalta and M. Guzmán-Mendoza, "Parametric assessment of the effect of oxygenated low carbon fuels in a light-duty compression ignition engine," *Fuel Processing Technology,* vol. 229, no. May, p. 107199, 2022.

[50] OPEL, *New Opel Movano-e,* OPEL, 2021.

[51] A. García, J. Monsalve-Serrano, D. Villalta and M. Guzmán-Mendoza, "OMEx Fuel and RCCI Combustion to Reach Engine-Out Emissions Beyond the Current EURO VI Legislation," *SAE Technical Paper,* no. 2021-24-0043, 2021.

[52] A. Al-Samari, "Study of emissions and fuel economy for parallel hybrid versus conventional vehicles on real world and standard driving cycles," *Alexandria Engineering Journal,* vol. 56, no. 4, pp. 721-726, 2017.

[53] Y. Huang, N. C. Surawski, B. Organ, J. Zhou, O. H. Tang and E. F. Chan, "Fuel consumption and emissions performance under real driving: Comparison between hybrid and conventional vehicles," *Science of The Total Environment,* vol. 659, no. April, pp. 275-282, 2019.

[54] T. Liu, W. Tan, X. Tang, J. Zhang, Y. Xing and D. Cao, "Driving conditions-driven energy management strategies for hybrid electric vehicles: A review," *Renewable and Sustainable Energy Reviews,* vol. 151, no. November, p. 111521, 2021.

[55] I. Taymaz and M. Benli, "Emissions and fuel economy for a hybrid vehicle," *Fuel,* vol. 115, no. January, pp. 812-817, 2014.

[56] A. García, J. Monsalve-Serrano, D. Villalta, M. Guzmán, P. Gaillard, F. Pesce, A. Vassallo, R. Durrett, M. Potter, M. Gonzalez and P. Najt, "Effects of Different Low Carbon Fuels on Performance and Emissions of Compression Ignition Engines," in *30th Aachen Colloquium Sustainable Monility 2021*, Aachen, 2021.

Abbreviations

BMEP	Brake mean effective pressure
CI	Compression ignition
DOC	Diesel oxidation catalyst
DOE	Design of experiments
DPF	Diesel particulate filter
EV	Electric vehicle
FAME	Fatty acid methyl esters
GBE	Gross brake efficiency

HC	hydrocarbons
HVO	Hydrogenated vegetable oil
ICE	Internal combustion engine
LCF	Low carbon fuel
LHV	Lower heating value
OEM	Original equipment manufacturer
PM	Particulate matter
PRR	Pressure rise rate
SI	Spark ignition
SOI	Start of injection
TTW	Tank-to-wheel
WLTC	World harmonized Light vehicle Test Cycle
WLTP	World harmonized Light vehicle Test Procedure
WTT	Well-to-tank
WTW	Well-to-wheel